Chapter 11

Quantitative Analysis of Subcellular Distribution of the SUMO Conjugation System by Confocal Microscopy Imaging

Abraham Mas, Montse Amenós, and L. Maria Lois

Abstract

Different studies point to an enrichment in SUMO conjugation in the cell nucleus, although non-nuclear SUMO targets also exist. In general, the study of subcellular localization of proteins is essential for understanding their function within a cell. Fluorescence microscopy is a powerful tool for studying subcellular protein partitioning in living cells, since fluorescent proteins can be fused to proteins of interest to determine their localization. Subcellular distribution of proteins can be influenced by binding to other biomolecules and by posttranslational modifications. Sometimes these changes affect only a portion of the protein pool or have a partial effect, and a quantitative evaluation of fluorescence images is required to identify protein redistribution among subcellular compartments. In order to obtain accurate data about the relative subcellular distribution of SUMO conjugation machinery members, and to identify the molecular determinants involved in their localization, we have applied quantitative confocal microscopy imaging. In this chapter, we will describe the fluorescent protein fusions used in these experiments, and how to measure, evaluate, and compare average fluorescence intensities in cellular compartments by image-based analysis. We show the distribution of some components of the *Arabidopsis* SUMOylation machinery in epidermal onion cells and how they change their distribution in the presence of interacting partners or even when its activity is affected.

Key words Subcellular localization, Confocal microscopy, Fluorescence, Intensity, Quantification, SUMOylation

1 Introduction

Subcellular localization is essential to protein function since it determines the access of proteins to interacting partners and post-translational modification machineries and enables the integration of proteins into functional biological networks [1].

Fluorescence microscopy is a powerful tool to study subcellular localization, protein–protein interactions, and intracellular dynamics of fluorophore tagged proteins [2]. The use of the green fluorescent protein (GFP) and its variants for generation of fluorescent fusion proteins facilitates the in vivo analysis of protein

L. Maria Lois and Rune Matthiesen (eds.), *Plant Proteostasis: Methods and Protocols,* Methods in Molecular Biology, vol. 1450, DOI 10.1007/978-1-4939-3759-2_11,

dynamics relevant to cell biological processes [3]. Usually, for analysis of subcellular localization, the translational fusion of the protein of interest with a fluorescent protein is transiently expressed in plants cells and examined with confocal microscopy.

The subcellular distribution of many proteins can be influenced by binding to other biomolecules and by posttranslational modification, including SUMOylation, phosphorylation, acetylation, ubiquitylation, farnesylation, and proteolytic processing [1]. When subcellular redistribution is only partial, changes in fluorescence intensity in specific cellular components could be difficult to visually distinguish and, to circumvent this limitation, it is highly recommended to include quantitative evaluation of fluorescence images [4]. However, few works have addressed how to obtain accurate data of protein subcellular localization by quantitative confocal microscopy analysis, since the majority of subcellular localization studies have been qualitative in nature and nonrelated to plant cell biology research.

SUMO (Small Ubiquitin-like MOdifier) is a small protein that is covalently attached to lysine residues of target proteins via a reversible posttranslational modification. SUMO attachment is regulated by the sequential action of the heterodimer SUMO-activating E1-enzyme (SAE2/SAE1), the SUMO-conjugating E2-enzyme (SCE1), and E3-ligase enzymes [5]. As protein modifier, SUMO modulates protein activity through regulation of subcellular localization, protein activity and stability, and protein–protein interactions [6]. SUMOylation occurs predominantly in the nucleus, but nonnuclear proteins have also been identified as SUMO conjugation targets [7]. However, it is unclear whether SUMOylation enzymes are translocated out of the nucleus to catalyze SUMOylation in other cellular compartments. Interestingly, in mammals, both SUMO-E1 activating enzyme subunits have distinct functional nuclear localization signals, NLSs, although the NLS present at the E1 large subunit Uba2 is the only one required for the efficient import of the E1 complex into the nucleus [8]. Moreover, regulation of *Hs*E1 localization has been proposed to be also dependent on posttranslational modification by SUMO at the C-terminal domain, which would be required for its nuclear retention [9]. In addition to the SUMO machinery components, SUMO can modulate substrate subcellular localization through covalent modification of the substrate, or through noncovalent interactions mediated by SUMO interacting motifs, SIM, in the protein target, or both. A well reported example of subcellular distribution regulation by SUMO is the tumor suppressor PML. PML localizes in nuclear bodies and, in addition to be modified by SUMO, it contains a SUMO binding motif that is independent of its SUMOylation sites and necessary for nuclear bodies localization [10].

In plants, SUMO conjugation has been involved in the regulation of abiotic stress and defense responses, plant development,

and flowering [11]. The Arabidopsis SUMO E1-activating enzyme displays nuclear localization like their human and yeast orthologues, consistent with the nuclear enrichment of SUMO targets identified in different studies [12, 13]. The E1 nuclear localization is determined by a conserved NLS located at the SAE2 E1-large subunit C-terminal tail [14]. Other members of the SUMOylation machinery are also localized to the nucleus, such as the SIZ1 E3 ligase that is present in the nucleoplasm and nuclear bodies [15]; the SUMO protease ESD4 that is enriched at the periphery of the nucleus [16]; and the SUMO proteases OST1 and OST2 that also localize to the nucleus, although OST1 is exclusively localized to the nucleoplasm while OST2 displays a nuclear punctuate pattern [17]. Other members of the SUMOylation machinery display a localization distributed among the nucleus and the cytosol such as SUMO1/2 [18], the E2 conjugating enzyme [18], and the E3 ligase MMS21 [19].

This protocol describes in detail a confocal image-based method to quantify and analyze the subcellular localization of some of the Arabidopsis SUMOylation machinery components. Specifically, we show that subcellular distribution of the SUMO E2-conjugating enzyme SCE1 is sensitive to its catalytic activity and to coexpression with SUMO1. We show that SCE1 was localized preferentially in the nucleus but could be also found in the cytosolic compartment. A point mutation in the SCE1 catalytic site, SCE1C94S, prevented efficient nuclear localization, suggesting a possible coupling of the catalytic activity to subcellular distribution. On the contrary, when SCE1 and SUMO1 were coexpressed, both proteins strongly colocalized in the nucleus and a significant signal reduction was observed in the cytosol. The quantitative analysis of the obtained confocal images allowed the statistical analysis of the observed subcellular protein dynamics. In this protocol, we describe the methods involving in vivo transient protein expression, image acquisition, quantification, and statistical analysis.

2 Materials

2.1 Vectors

All constructs were previously generated [18] and the map is shown in Fig. 1.

1. pWEN24 encoding ECFP.
2. pWEN25 encoding EYFP.
3. pWEN24 encoding the protein fusion ECFP:SUMO1 mature form (Met1-Gly93).
4. pWEN25 encoding the protein fusion EYFP:SCE1.
5. pWEN25 encoding the protein fusion EYFP:SCE1 catalytic inactive form C94S.

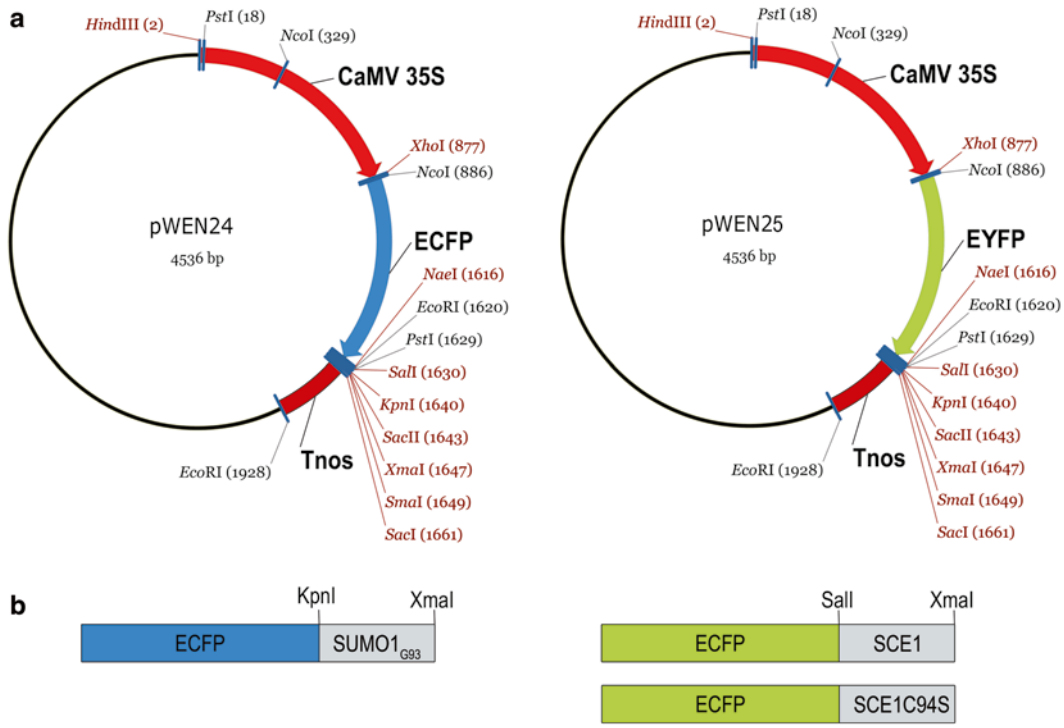

Fig. 1 Constructs used in this protocol for biolistic transient transformation. (**a**) pWEN24 (encoding the ECFP) and pWEN25 (encoding the EYFP) vectors were used as FP localization controls, and they were used for generating the ECFP::SUMO1, ECFP::SCE1, and ECFP::SCE1C94S protein fusion variants. The schematic representation of the protein fusions expressed in onion cells in this protocol are shown in panel (**b**)

2.2 Plant Tissue

Epidermis from inner onion leaves obtained at local stores (*see* **Note 1**).

2.3 Bombardment Equipment

1. PDS-1000/He System (BIO-RAD) Biolistic Particle Delivery System.
2. Macrocarriers Ref. 1652335, BIO-RAD.
3. Macrocarriers holders Ref. 1652322, BIO-RAD.
4. 1100 psi rupture disks Ref. 1652326, BIO-RAD.
5. Stopping screens Ref. 1652336, BIO-RAD.
6. Tungsten M17-Microcarriers Ref. 1652268, BIO-RAD.

2.4 Reagents

1. Pure Yield™ Plasmid Midiprep System (Promega) or similar.
2. Calcium Chloride Ref. C-4901 (Sigma Aldrich).
3. Spermidine Ref. S2626 (Sigma Aldrich).
4. Ethanol absolute, reagent grade ACS, ISO (Scharlau).

2.5 Microscopy Equipment

1. Surgical blades.
2. Microscope slides and cover slips.
3. Leica SPS confocal Laser Scanning Microscope.

2.6 Software

1. Leica SPS confocal software.
2. ImageJ freeware (http://rsbweb.nih.gov/ij/) and MS Excel.

3 Methods

3.1 Design and Generation of Fluorescence Chimeric Proteins

Choose a fluorescence protein for protein fusion chimera construction according to the available image acquisition equipment, biological sample restrictions, structural and functional organization of the protein of interest, and experimental design. The Green Fluorescence Protein (GFP) and its color genetic variants, as for example Yellow Fluoresce Protein (YFP), Cyan Fluorescence Protein (CFP), or Red Fluorescence Protein (RFP), are widely used in subcellular localization studies. Instruments with simple optical setup can easily distinguish between fluorescence proteins having none or minimal emission overlaps. We used as example (ECFP/EYFP) for the subcellular localization quantification of our proteins of interest as described in **item 2.1**, Subheading 2 (*see* **Note 2**).

Proteins of interest were fused at the C-terminus of fluorescent protein using standard molecular biology techniques. As for SUMO1, only N-terminal fusions (ECFP:SUMO) can be performed since the C-terminal fusion (SUMO:ECFP) would generate a nonconjugable SUMO form that could result in localization artifacts (*see* **Note 3**). Protein fusion expression was regulated by the strong and constitutive CaMV 35S promoter.

3.2 Biolistic Bombardment: Microcarrier Preparation

All steps were performed at room temperature and nonsterile conditions. Purity of used reagents meets the ACS reagent grade.

1. Weigh out 60 mg of microparticles into a 1.5 ml microfuge tube.
2. Add 1 ml of 70% ethanol (v/v).
3. Vortex vigorously for 3–5 min (a platform vortex is useful).
4. Allow the particles to soak in 70% ethanol for 15 min.
5. Pellet the microparticles by spinning for 5 s in a microfuge.
6. Remove and discard the supernatant.
7. Add 1 ml of autoclaved water in order to wash microparticles.
8. Vortex vigorously for 1 min.
9. Allow the particles to settle for 1 min.
10. Pellet the microparticles by briefly spinning in a microfuge.
11. Remove the liquid and discard.
12. Repeat **7**–**11** two additional times.
13. After the third wash, add 1 ml of sterile 50% glycerol to bring the microparticle concentration to 30 mg/ml (*see* **Note 4**).

3.3 Biolistic Bombardment: Coating Washed Microcarriers with DNA

1. Vortex prepared microcarriers for 5 min on a platform vortex to resuspend and disrupt agglomerated particles (*see* **Note 5**).
2. Transfer 12.5 µl of microcarriers to a 1.5 ml microcentrifuge tube.
3. Add 1–2 µg of DNA in a maximum volume of 2–3 µl (*see* **Note 6**).
4. Add the precipitation solution (12.5 µl 2.5 M $CaCl_2$ and 5 µl of 0.1 M spermidine) (*see* **Note 7**).
5. Vortex vigorously for 3 min.
6. Allow the particles to settle for 1 min.
7. Pellet the microcarriers by spinning 5 s in a microfuge.
8. Remove the supernatant and discard.
9. Add 200 µl of 70% ethanol.
10. Pellet the microcarriers by spinning 5 s in a microfuge.
11. Remove the supernatant and discard.
12. Add 200 µl of 100% ethanol.
13. Pellet the microcarriers by spinning 5 s in a microfuge.
14. Remove the supernatant and discard.
15. Add 20 µl of 100% ethanol.
16. Gently resuspend the pellet by tapping the side of the tube several times, followed by vortexing for 2–3 s (*see* **Note 8**).

3.4 Performing Bombardment

1. Prepare the onion samples by cutting the fresh inner leaves of the onion. Prepare three leaves for performing a triplicate transformation of each DNA sample.
2. Place the macrocarrier into the macrocarrier holder. Load 6 µl of microcarriers coated with DNA onto a macrocarrier. Prepare macrocarrier triplicates for each DNA sample (*see* **Note 9**).
3. Transfer selected macrocarriers to individual Petri dishes for easier handling.
4. Check helium supply, 200 psi in excess of desired rupture pressure (*see* **Note 10**).
5. Turn on the vacuum source and power ON the PDS-1000/He unit (*see* **Note 11**).
6. Load the rupture disk into retaining cap and tighten with torque wrench.
7. Load macrocarrier and stopping screen into the microcarrier launch assembly.
8. Place microcarrier launch assembly and target tissue in chamber and close door (*see* **Note 12**).
9. Generate vacuum in the chamber until a 27-mmHg (0.063 atm) pressure is reached and hold it (*see* **Note 13**).

10. Fire button continuously depressed until rupture disk burst and release Fire button (*see* **Note 14**).
11. Release vacuum from chamber.
12. Remove target tissue from chamber and unload macrocarrier, stopping screen from microcarrier launch assembly and broken rupture disk.
13. Repeat **steps 6–12** for each replicate.
14. Remove helium pressure from the system (after all experiments are completed).
15. Place the onion leaves over filter paper soaked in water and wrap in aluminum foil. Leave it at room temperature in the dark.

3.5 Fluorescence Protein Detection and Imaging

1. Screen plant samples under a fluorescence stereomicroscope to check if transient expression was successful 16 h after bombarding.
2. Cut with surgical blades an appropriate onion leaf piece containing cells exhibiting strong fluorescence, as a result of having a good transformation rate and expression level.
3. Remove the epidermal cell layer of the selected onion leaf area and place it on a microscopic slide containing a drop of water. Cover with a cover slip.
4. Set up all the hardware parameters and imaging settings of your confocal laser scanning microscope, and activate the sequential mode imaging in order to collect the fluorescence of coexpressed fluorophores independently (*see* **Note 15**).
5. Place the microscopic slide under a 20× objective in the confocal microscope in order to observe complete single onion cells.
6. Take a z-stack of a cell fixing the upper and lower limits of the z-series with a step size of 1 μm to reach the maximum cell depth (Fig. 2a) The maximum cell depth of the z-series is defined as the depth necessary for covering the maximum cell area and the whole nuclear volume (*see* **Note 16**).
7. Monitor image saturation degree under the imaging settings selected for EYFP imaging. Select HiLo Lut mode and scan the defined maximum cell depth for detecting saturated pixels, which appear highlighted on the screen.
8. Adjust gain parameter for generating an image displaying the minimum saturated pixels that ensure the full range quantification from 0 to 65553 in a 16 bit color depth. The presence of a portion of saturated pixels is necessary when comparing cell compartments displaying large differences in fluorescence intensities, such as nucleus versus cytosol, in order to measure significant fluorescence signal from the compartment exhibiting less intensity (the cytosol in this case).

9. Repeat **steps 7–8** for ECFP imaging.
10. Collect the z-stack series for EYFP, ECFP, and transmission light.

3.6 Average Fluorescence Intensity Measurements

1. Open collected z-stack image series with ImageJ software using split channel mode (http://rsbweb.nih.gov/ij/).
2. In the main menu, select the *image/stacks/z-projection/max intensity* option for generating the maximum projection of the z-series corresponding to the cell being analyzed (Fig. 2b) (*see* **Note 17**).
3. Check the nucleus saturation pixel degree: draw a circular region of interest (ROI) comprising the whole nucleus by using the freehand selection tool, open the *analyze/histogram* window (Ctrl + H) and determine the portion of saturated pixels contained in the ROI (Fig. 2c) We used as a criterion not analyzing images displaying fluorescence saturation for more than 20% of captured pixels (we estimate that pixels contained in the final upper bin of the histogram display fluorescence saturation or are very close to it) (Fig. 2d) (*see* **step 8** in Subheading 3.3).
4. With the *drawing/freehand selection tool*, draw in the maximum intensity projection image a first region of interest (ROI1) following the perimeter of the nucleus and click on the *Add button* on the *ROI manager* window. Then make a ROI2 enclosing cytosol but excluding the nucleus and click on the *Add button* on the *ROI manager* window. Finally, make a third ROI outside of the cell as a control of the background, for which we use the same area as the cytosol (Fig. 3a), click on the *Add button* on the *ROI manager* window. To analyze ROIs of the same size, for example cytosol and background, the selected ROI can be dragged with the cursor to other region of interest.
5. From the main menu open *Analyze/Set measurements* window and select *Area* and *Mean Gray Value* in the check box list (Fig. 3b). Next, open the ROI manager window (main menu\analyze\tools) and select both check boxes (show all and labels) (Fig. 3c) (*see* **Note 18**).
6. On the *ROI manager* window, select all generated ROIs and click on the *Measure button*. The Results window containing the information regarding the Areas and Average intensities for the selected ROIs will open (Fig. 3d).

3.7 Statistical Analysis of Average Fluorescence Intensity

The average fluorescence intensity in specific cellular compartments such as nucleus and cytosol must be quantified for each cell as follows:

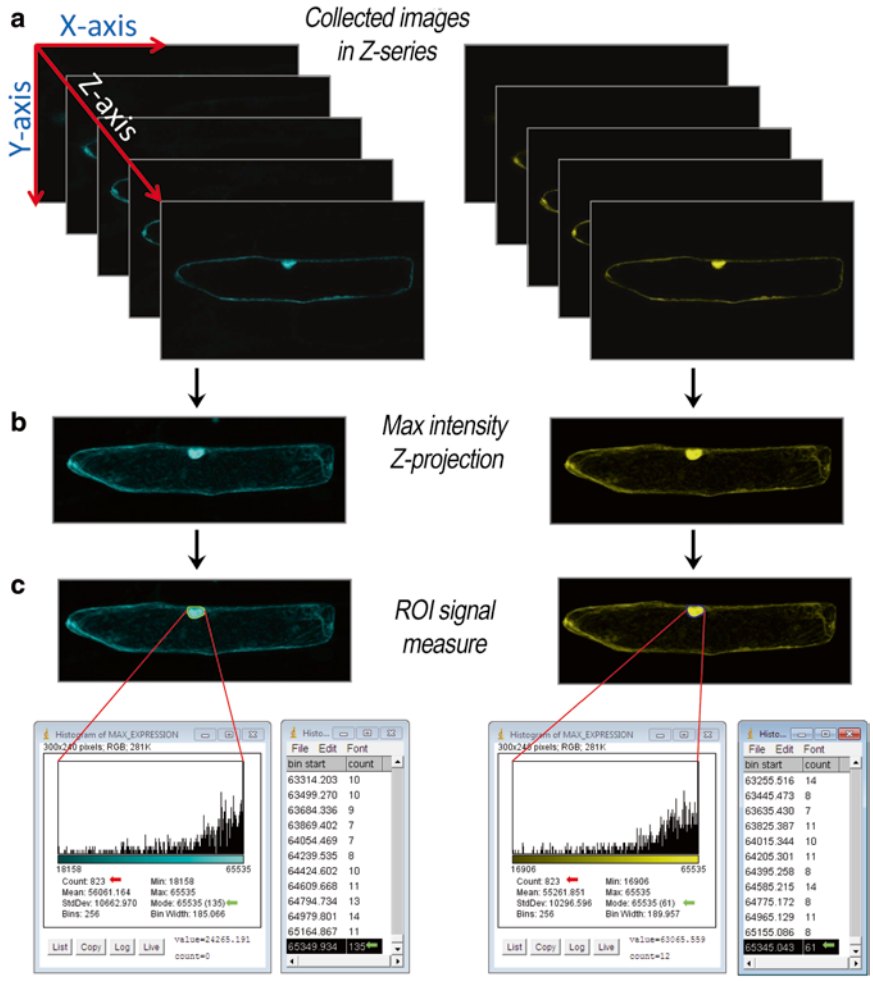

Fig. 2 Imaging of fluorescence protein detection. (**a**) Collected images in Z-series. (**b**) Maximum intensity Z-projection of the image stack. (**c**) The evaluation of nucleous saturation degree is estimated using the histogram tool. The histogram is built counting 823 pixels (Count) distributed among 256 bins. (**d**) The saturation degree is calculated as the relation between the number of saturated pixels (pixels contained in the final upper bin; *green arrow*) and the total pixels (*red arrow*). For instance, in the case of the ECFP, 135 pixels displays intensities between 65349 and the upper limit 65535, comprising the 17.2 % of the total pixels

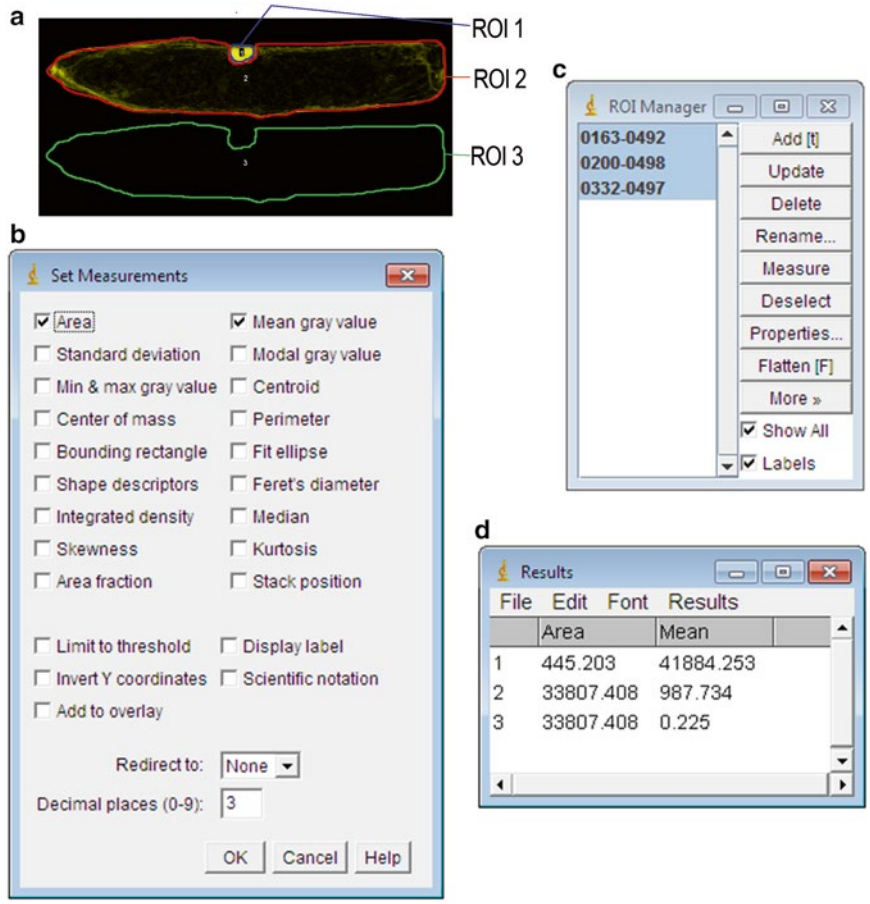

Fig. 3 Average fluorescence intensity measurement. (**a**) Multi ROI fluorescence intensity measurements by ImageJ. ROI1, nucleus. ROI2, cytosol. ROI 3, background. (**b**) *Set measurements* window. (**c**) *ROI manager* window with selected ROIs. (**d**) *Results* window displaying Area and mean intensity measurements of the selected ROIs

1. Copy data from **step 6** in Subheading 3.4 to an Excel file.
2. Remove the value of the background (BG) average to the nucleus and cytosolic mean intensity value.
3. Calculate the cytosolic and nuclear Integrated Density (ID) as the product of the cytosol or nuclear Area and the corrected Mean intensity without the background (*see* **Note 19**).

$$\mathrm{ID}_{\mathrm{nucleus}} = \mathrm{ROI1\ area} \times \left(\mathrm{ROI1\ mean\ intensity} - \mathrm{ROI3\ background\ intensity}\right)$$

$$\mathrm{ID}_{\mathrm{cytosol}} = \mathrm{ROI2\ area} \times \left(\mathrm{ROI2\ mean\ intensity} - \mathrm{ROI3\ background\ intensity}\right)$$

4. Calculate the Cytosol Fluorescence Ratio. In order to compare between different transformed cells, the Cytosol Fluorescence Ratio is calculated as a measure of the cytosolic signal enrichment.

$$\text{Cytosol Fluorescence Ratio} = \frac{\text{ID}_{\text{cytosol}}}{\text{ID}_{\text{nucleus}} + \text{ID}_{\text{cytosol}}}$$

At least seven cells must be analyzed in each transformation experiment.

5. Repeat **steps 1–3** for each fluorescence channel analyzed.
6. Calculate and plot the average of all obtained ratios and the corresponding standard errors (*see* **Note 20**).

As a practical example for the present protocol, we have analyzed the quantitative subcellular distribution of the SUMO E2 conjugating enzyme, SCE1, and evaluated the effect of SUMO coexpression and/or its catalytic activity on its localization. In Fig. 4, we show that SCE1 was localized preferentially in the nucleus but could also be found in the cytosolic compartment, consistent with a potential role for SCE1 in SUMOylating cytoplasmic proteins. A point mutation in the SCE1 catalytic site, SCE1C94S, prevented efficient nuclear localization, suggesting a possible coupling of catalytic activity to cellular localization. On the contrary, when SCE1a was coexpressed with SUMO1, both proteins colocalized strongly in the nucleus, with little signal detected in the cytoplasm. The effect of SUMO1 on SCE1 nuclear enrichment is not observed when the activity mutant SCE1C94S was coexpressed with SUMO, supporting a potential coupling of the catalytic activity to cellular localization (Fig. 4a). These observations were supported by quantitative data obtained applying the present protocol (Fig. 4b).

4 Notes

1. For biolistic bombardment assay we recommend to used fresh inner onion leaves as plant tissue because it is easy to obtain and, after peeling, it provides living cells in a monolayer, which facilitates confocal microscopy imaging. The cells of this tissue can be efficiently transformed since the microcarriers bombardment can be spread over a large homogenous area, without nonoverlying cell layers intercepting some of the particles delivered. Moreover, this tissue consists of large cells containing big nucleus and cytosol and, more interestingly, no chlorophyll interference, which make them easy to analyze. Alternatively, *Arabidopsis* roots are also suitable for this technique.
2. Optimal transformation and expression efficiency is obtained by using small plasmids such as the ones proposed in this protocol.
3. In absence of information about structural and functional protein organization, protein fusions should be performed at FP

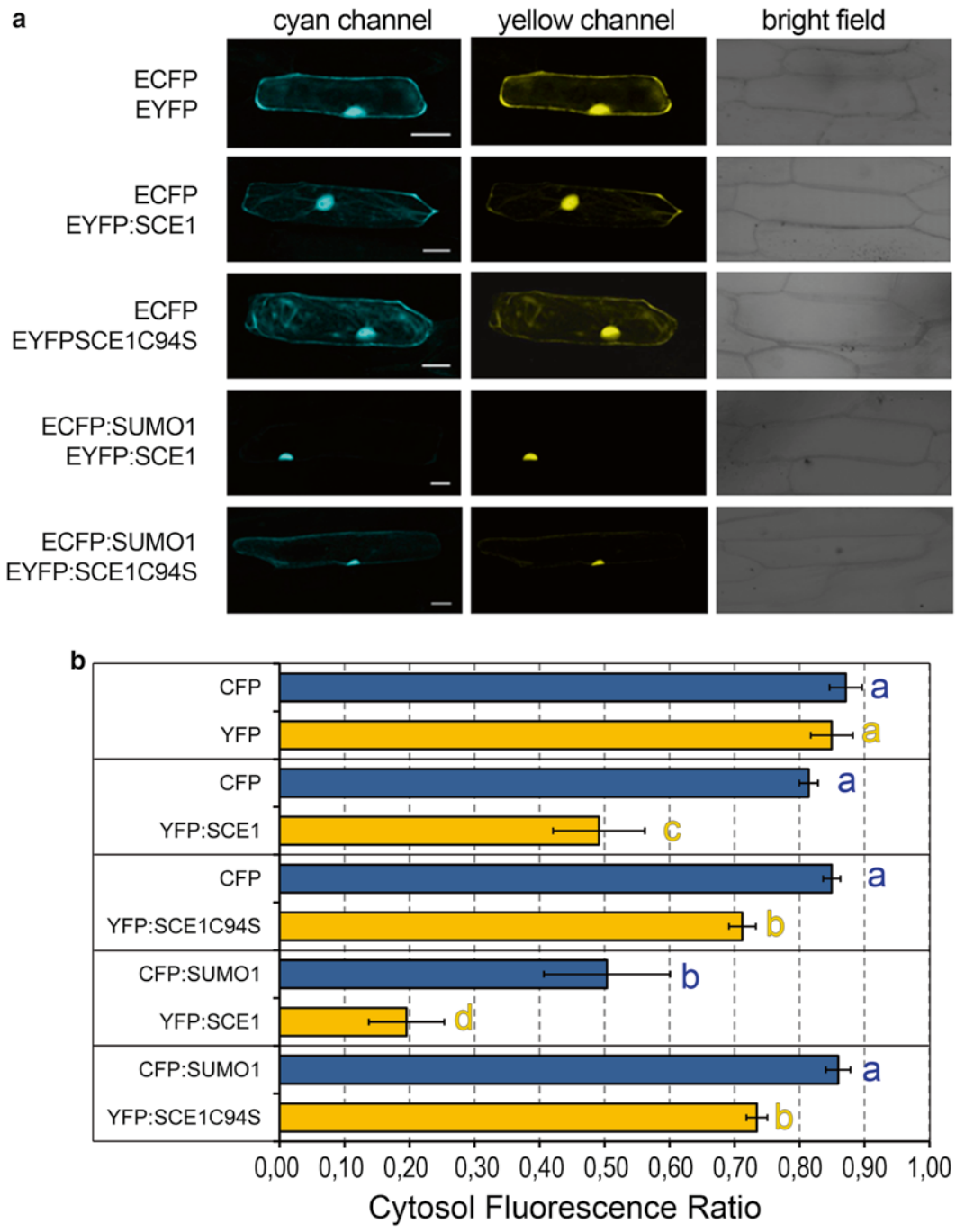

Fig. 4 Subcellular localization of *Arabidopsis* SCE1 and SUMO1. (**a**) Epidermal onion cells were transiently transformed with vectors expressing the following fluorescence proteins as indicated on the left: EYFP + ECFP, ECFP + EYFP:SCE1, ECFP + EYFP:SCEC94S catalytic mutant, ECFP:SUMO1 + EYFP:SCE1, and ECFP:SUMO1 + EYFP:SCE1C94S catalytic mutant. Bars = 50 μm. (**b**) Cytosol Fluorescence Ratio was measure for at least seven cells in each experiment as indicated in the present protocol. Average values and standard error are shown in the plot. *T*-test was performed for each fluorophore and *letters* next to the bars indicate those proteins displaying a significant distinct subcellular localization ($p \leq 0.02$)

C-terminus and N-terminus to corroborate that localization is not affected by the position of the fluorescent protein.

4. Tungsten aliquots should be stored at −20 °C to prevent oxidation. Avoid using old aliquots which will reduce the transformation efficiency of the assay.
5. When removing aliquots of microcarriers, it is important to continuously vortex the tube containing the microcarriers to maximize uniform sampling. When pipetting aliquots, hold the microcentrifuge tube firmly at the top while continually vortexing the base of the tube.
6. In the case of a cotransformation, for allowing equal transformation efficiency, both plasmids must be mixed before adding the microcarriers to the DNA sample. It is also desirable to use plasmids of similar size.
7. It is highly recommended to handle spermidine in one-use aliquots since freezing can affect its stability as well as transformation efficiency of the assay.
8. The DNA-coated microcarriers can be stored at −20 °C for few days, although is better to use it immediately.
9. The edge of the macrocarrier should be securely inserted under the lip of the macrocarrier holder. In case that there are not enough macrocarrier holders for all the samples, DNA-coated microcarriers can be loaded on the macrocarrier and transfer to the holder before performing the bombardment (in this case, we keep the prepared macrocarriers in Petri dishes labeled according to the DNA construct used).
10. 1100 psi rupture disks are recommended for plant tissues so the helium supply should have a pressure of 1300 psi.
11. It is recommended that vacuum generation and release are performed at the highest speed.
12. One of the most important parameters to optimize is target shelf placement within the bombardment chamber. This placement directly affects the distance that the microcarriers travel to the target cells for microcarrier penetration and transformation. We recommend starting with the closest second position to the stopping screen.
13. Set the vacuum switch on the PDS-1000/He (middle red control switch) to VAC position. When the desired vacuum level is reached, hold the camber vacuum at that level by quickly pressing the vacuum control switch through the middle VENT position to the bottom HOLD position.
14. With the vacuum level in the bombardment chamber stabilized, press and hold the FIRE switch to allow helium pressure to build inside the gas acceleration tube that is sealed by a selected rupture disk. A small pop will be heard when the rupture

disk burst. The rupture disk should burst within 10% of the indicated rupture pressure and within 11–13 s. Release the FIRE switch immediately after the disk ruptures to avoid wasting helium.

15. For accurate quantitative evaluation and comparison of average fluorescence intensities, we recommend using a confocal microscopy with high chromatic resolution with 16 Bits and 65535 grey levels. It is also highly recommended to take images with the same hardware parameters such as objective, laser power, pinhole opening, gain, offset values, and zoom factor as well as to prepare and analyze all experimental variants at the same time under the same conditions. All of this will allow reducing the influence of experimental conditions on the fluorescence intensity measurement and quantification. Regarding to laser power, adjust the intensity in order to avoid photodamage and photobleaching of the fluorescence. Try to use the minimum amount of laser power to get sufficient signal at gain levels that not result in too much background (700–800av). To enhance the quality of your image acquisition, a double scan or an average line of two from the image acquisition set up is recommended since it will diminish the background. The pinhole aperture can be increased if photodamage is observed due to laser illumination or if electronic noise occurs when the photomultiplied gain is increased. Take into account that the more you open the pinhole the more noise fluorescence you have, loosing confocality.
16. To eliminate the influence of the imaging depth on the fluorescence intensity, avoid plant cells with the nucleus located deeper, and start the z-series from the surface of the cell, otherwise the quality of images collected from deeper layers is worse due to the dispersion of laser light and the quantification and comparison of fluorescence intensity will be not appropriate. We have consider the maximum cell depth of the z-series as the depth necessary for covering the maximum cell area and the whole nuclear volume since we assume that half of the cell is more or less symmetrical to the other half. The main advantage of this maximum cell depth set up consists in a reduction of layer number in the z-series, which translates into shorter acquisition time and fluorescence photobleaching decrease.
17. In this method we perform the fluorescence intensity quantification in a maximum intensity projection, which is defined as an output image each of whose pixels contains the maximum value over all images in the stack at the particular pixel location.
18. The area is defined as the area of selection in square pixels. The Mean Grey Value, or average intensity, is the sum of the gray values of all the pixels in the selection divided by the number of pixels.

19. Integrated Density (ID) is an appropriate descriptor that allows comparing the cytosolic and nucleus intensity within cells with different size.
20. Perform statistical analysis applying the T-test (significant differences are considered when $p \leq 0.02$).

Acknowledgments

This work was supported by the European Research Council (grant ERC-2007-StG-205927) and Departament d'Innovació, Universitats i Empresa from the Generalitat de Catalunya (Xarxa de Referència en Biotecnologia and 2014SGR447). A.M. was supported by predoctoral fellowships FPU12/05292. This article is based upon work from COST Action (PROTEOSTASIS BM1307), supported by COST (European Cooperation in Science and Technology). We thank Reyes Benlloch for critical reading.

References

1. Hung MC, Link W (2011) Protein localization in disease and therapy. J Cell Sci 124(Pt 20):3381–3392. doi:10.1242/jcs.089110
2. Waters JC (2009) Accuracy and precision in quantitative fluorescence microscopy. J Cell Biol 185(7):1135–1148. doi:10.1083/jcb.200903097
3. Hanson MR, Kohler RH (2001) GFP imaging: methodology and application to investigate cellular compartmentation in plants. J Exp Bot 52(356):529–539
4. Lichocka M, Schmelzer E (2014) Subcellular localization experiments and FRET-FLIM measurements in plants. Bio Protoc 4(1):e1018, http://www.bio-protocol.org/e1018
5. Ulrich H (2009) The SUMO system: an overview. In: Ulrich H (ed) SUMO protocols, vol 497, Methods in molecular biology. Humana Press, Totowa, NJ, pp 3–16. doi:10.1007/978-1-59745-566-4_1
6. Wilkinson KA, Henley JM (2010) Mechanisms, regulation and consequences of protein SUMOylation. Biochem J 428(2):133–145
7. Wasik U, Filipek A (2014) Non-nuclear function of sumoylated proteins. Biochim Biophys Acta 1843(12):2878–2885. doi:10.1016/j.bbamcr.2014.07.018
8. Moutty MC, Sakin V, Melchior F (2011) Importin alpha/beta mediates nuclear import of individual SUMO E1 subunits and of the holo-enzyme. Mol Biol Cell 22(5):652–660
9. Truong K, Lee TD, Li BZ, Chen Y (2012) Sumoylation of SAE2 C terminus regulates SAE nuclear localization. J Biol Chem 287(51):42611–42619. doi:10.1074/jbc.M112.420877
10. Shen TH, Lin HK, Scaglioni PP, Yung TM, Pandolfi PP (2006) The mechanisms of PML-nuclear body formation. Mol Cell 24(3):331–339. doi:10.1016/j.molcel.2006.09.013
11. Lois LM (2010) Diversity of the SUMOylation machinery in plants. Biochem Soc Trans 38(Pt 1):60–64. doi:10.1042/BST0380060
12. Miller MJ, Scalf M, Rytz TC, Hubler SL, Smith LM, Vierstra RD (2013) Quantitative proteomics reveals factors regulating RNA biology as dynamic targets of stress-induced SUMOylation in Arabidopsis. Mol Cell Proteomics 12(2):449–463
13. Miller MJ, Barrett-Wilt GA, Hua Z, Vierstra RD (2010) Proteomic analyses identify a diverse array of nuclear processes affected by small ubiquitin-like modifier conjugation in Arabidopsis. Proc Natl Acad Sci U S A 107:16512
14. Castaño-Miquel L, Seguí J, Manrique S, Teixeira I, Carretero-Paulet L, Atencio F, Lois LM (2013) Diversification of SUMO-activating enzyme in arabidopsis: implications in SUMO conjugation. Mol Plant 6(5):1646–1660. doi:10.1093/mp/sst049
15. Miura K, Rus A, Sharkhuu A, Yokoi S, Karthikeyan AS, Raghothama KG, Baek D, Koo YD, Jin JB, Bressan RA, Yun DJ, Hasegawa PM (2005) The Arabidopsis SUMO E3 ligase SIZ1 controls phosphate deficiency responses.

Proc Natl Acad Sci U S A 102(21): 7760–7765

16. Murtas G, Reeves PH, Fu YF, Bancroft I, Dean C, Coupland G (2003) A nuclear protease required for flowering-time regulation in Arabidopsis reduces the abundance of SMALL UBIQUITIN-RELATED MODIFIER conjugates. Plant Cell 15(10):2308–2319
17. Conti L, Price G, O'Donnell E, Schwessinger B, Dominy P, Sadanandom A (2008) Small ubiquitin-like modifier proteases OVERLY TOLERANT TO SALT1 and -2 regulate salt stress responses in Arabidopsis. Plant Cell 20(10):2894–2908
18. Lois LM, Lima CD, Chua NH (2003) Small ubiquitin-like modifier modulates abscisic acid signaling in Arabidopsis. Plant Cell 15(6): 1347–1359
19. Huang L, Yang S, Zhang S, Liu M, Lai J, Qi Y, Shi S, Wang J, Wang Y, Xie Q, Yang C (2009) The Arabidopsis SUMO E3 ligase AtMMS21, a homologue of NSE2/MMS21, regulates cell proliferation in the root. Plant J 60(999A): 666–678